Study on scaling analysis methods based on Lead-Bismuth loop with natural circulation*

Jianing Xu,[1,2] Zhen Wang,[1,†] Rui Pan,[1] Shichao Zhang,[1] Qiusun Zeng,[1] and Jie Yu[1,2]

[1]*Institute of Nuclear Energy Safety Technology, Chinese Academy of Sciences, Hefei, 230031, China*
[2]*University of Science and Technology of China, Hefei 230026, China*

The natural circulation capability of the lead-bismuth eutectic (LBE) is outstanding and its use as the coolant is beneficial for improving the efficiency and passive safety of the advanced nuclear reactors. The scaled-down experimental facilities play an important role in further evaluating the natural circulation of lead-bismuth. Traditional studies of the scaling methods are carried out for water-cooled reactors. To provide the theory for the design of the scaled experimental facilities and further verify the traditional scaling methods for LBE flow, multiple methods such as H2TS and DSS were applied to an LBE loop in this study. A simplified single-phase natural circulation case was established using the Relap5 code and the corresponding criteria were deduced based on the different scaling methods. The study analyzed the steady and transient cases and the characteristics of several methods were compared. The results indicate that the H2TS and DSS methods can accurately simulate the steady cases of natural circulation in the LBE loops. For the transient conditions with power changes, the DSS method can simulate the initial stage of the dynamic process more accurately when the length ratio is small. As the length ratio increases, the transient deviation of all methods is reduced. In addition, when the power changes nonlinearly, the model obtained by the DSS method is more consistent with the prototype case than the H2TS method.

Keywords: Lead-bismuth eutectic; Lead-based fast reactor; Natural circulation; Scaling analysis method

Nomenclature

List of symbols

l	LBE circulation length
A	Cross-section area
w	Mass flow rate
t	Time
g	Gravity acceleration
ΔT	Temperature difference
H	Height between cooling heating section center
f	Friction loss coefficient
d	Inner pipe diameter
k	Form loss coefficient
c_p	Specific heat capacity at constant pressure
T	Temperature
u	Fluid velocity
q	Heat flux
z	Axial length of heating section
Q	Core power

Greek symbols

β_s	Thermal expansion coefficient
ρ	Density
ξ	Wetted perimeter
ω	Normalized sum of agents-of-change
β	Normalized conserved quantity
τ_s	Process time interval
λ	Constant scale factor

Subscripts

R	Ratio between the model and prototype
P	Prototype
M	Model

Abbreviations

Ri	Richardson number
Fr	Friction number
Qs	Heat source number

* Supported by the National Key R & D Program of China under the Grant No. 2022YFB1902503 and the Youth Innovation Promotion Association of Chinese Academy of Sciences (CAS) under the Grant No.2023466.

† Corresponding author, Zhen Wang, Institute of Nuclear Energy Safety Technology, Chinese Academy of Sciences, Hefei, 230031, China, 15656920911, zhen.wang@inest.cas.cn

1. INTRODUCTION

The safe and efficient utilization of the nuclear energy is beneficial for the sustainable development of all countries. The nuclear technology has been continuously iterated, and the concept of fourth-generation advanced reactors has been proposed. The heavy liquid metal LBE has a high boiling temperature, a moderate melting temperature, a high thermal conductivity, and outstanding heat transfer capacity[1–4]. Meanwhile, it can meet the reactor design requirements in terms of neutronic and safety characteristics. Therefore, the lead-cooled fast reactor has become one of the six fourth-generation reactors in the new century[5–7].

Natural circulation relies on the density difference between the hot and cold fluids to drive the flow of the coolant, which is beneficial for reducing the reactor's dependence on the active equipment[8]. It plays an important role in the passive safety of the nuclear reactors. The natural circulation ability of the liquid LBE is quite outstanding compared with the

water. This enhances the passive safety under the accident conditions and provides a new design concept for the reactors, which use natural circulation to drive the coolant under the normal operating conditions. Overall, this is conducive to the development of miniaturization and specialization of the reactors. Examples include the Small natural circulation lead-based fast reactor-10 (SNCLFR-10)[9, 10], Ubiquitous, Rugged, Accident-forgiving, Non-proliferating, and Ultra-lasting Sustainer (URANUS)[11],Lead-bismuth eutectic cooled fast reactor-180 (LFR-180) and China lead-alloy cooled research reactor-I (CLEAR-I)[12, 13]. Therefore, to develop the fast reactors further, it is necessary to analyze the natural circulation of LBE more comprehensively.

Many studies of the single-phase natural circulation of LBE have been reported in recent years. Ma et al.[14] used the Thermal-hydraulic ADS lead-bismuth loop (TALL) to investigate the transient conditions in the heavy liquid metal (HLM) cooled fast reactors. The ability and stability of the natural circulation were evaluated, and the influencing factors on the circulation characteristics were discussed simultaneously. Agostini et al.[15] used the Chemical operational transient (CHEOPE) loop to study the fluid flow from the force to natural circulation and verified the accuracy of the Relap5 calculation code in predicting the LBE mass flow rate. Coccoluto et al.[16] summarized the results of the experiments conducted on the Natural Circulation Experiment (NACIE) loop. On this basis, the Relap5 code was modified and validated to allow LBE as the coolant. Li et al. used the KYLIN-II facility to analyze the effects of heat power and secondary side flow rate on natural circulation and obtained the maximum flow rate of the facility at the rated power. In addition, the study validated the theoretical calculation formula for the flow rate[17, 18]. Shi et al.[19] achieved the gas lift circulation of LBE-argon in the natural circulation capability loop test facility, and showed the height of the riser is related to the circulation capacity of the gas lift pump. Then, the same facility was used to analyze the flow resistance and the heat transfer in the circulation channel[20]. Duan et al.[21] designed a new startup scheme for the SNCLFR-100 reactor and studied the flow instability in the startup phase. Yu et al.[22] carried out an uncertainty analysis of the overpower accident based on the lead-based natural circulation fast reactor and discussed the relevant factors influencing the transient safety.

Using a large amount of lead-bismuth for experiments may have high costs, and the issues like material corrosion also need to be considered. Using the water models to simulate heavy liquid metals is a suitable solution and has been applied within a certain range[23–25]. However, the relevant errors may be caused by the different thermal properties between water and LBE. Therefore, establishing a scaled-down lead-bismuth experimental facility using the scaling methods is also a feasible solution that integrates reliability, safety, and cost.

The scaling methods were commonly used for the water reactors in the previous studies and different methods have guided the design of many experimental facilities[26, 27]. For example, the Simulatore per Esperienze di Sicurezza-2 (SPES-2) and the Rig of Safety Assessment (ROSA) facilities were designed using the power-volume method[28, 29], the Purdue University multidimensional integral test assembly (PUMA) and the Advanced Thermal-hydraulic Test Loop for Accident Simulation (ATLAS) were designed using the three-level scaling method and the ACME was designed using the H2TS method[30, 32–34]. In addition, new methods such as the FSA and DSS have also been gradually proposed[35, 36]. Li et al[37–39]. used the scaling methods to analyze the distortion of the gravity-driven drainage process in recent years. Furthermore, based on the water loop, different strain transformations of the DSS method have been evaluated[40–42] and the relevant theories have been enriched.

In contrast, research on the scaling analysis of lead-bismuth is still relatively lacking. To further expand the application of the scaling methods in the LBE circulation and provide the basis for the design of the scaled experimental devices, the traditional H2TS and the innovative DSS methods have been applied to the natural circulation of LBE and the conclusions of the previous studies were compared to enrich the theories[9]. The natural circulation in the lead-bismuth fast reactor was simplified into a symmetrical rectangular loop, and the numerical model was established by using the Relap5/Mod4.0 code. Several methods were used and the corresponding model cases were established. The static and dynamic characteristics were analyzed and their errors were calculated. The applicability of varying scaling methods in the new field was evaluated and the differences among those methods were discussed.

2. PHYSICAL MODEL

2.1. LBE single-phase natural circulation loop

Fig. 1a shows the structure of the traditional lead-cooled reactor. When the main pump fails or the reactor is designed to operate in a passive mode, the heat of the core is removed by the natural circulation. Experimental loops were often used to simulate the LBE flow inside the reactors[14–17]. The simplification principles of the model are as follows:

(1) LBE flows along the uniform and adiabatic pipes within the experimental loop and the influence of the monitoring instruments was ignored.

(2) The Boussinesq hypothesis was applied to the facility and the impact of density changes on fluid characteristics was ignored[13].

(3) The core was regarded as a point heat source and the power was calculated based on the scaling methods.

A symmetrical loop was obtained as the prototype case for scaling analysis. The loop is illustrated in Fig. 1b. After flowing through the electric heater that simulates the reactor core, the LBE reached the top of the loop and it was divided into two parts to enter the symmetrical heat exchangers. The main parameters of the prototype loop are shown in Table 1.

Table 1. Design parameters of the prototype model under LBE natural circulation

Parameters	Value
Coolant	LBE
Pressure (MPa)	0.1
Total height (m)	2.1
Total width (m)	2.04
Pipe inner diameter (mm)	30
Heating section length (m)	0.4
Initial power (KW)	0-22

2.2. Node model of the LBE loop

The LBE loop shown in Fig. 1b was simulated using the Relap5/Mod4.0 code. After the relevant improvements, this code can conduct the thermal-hydraulic calculations for lead-bismuth fluids. The node diagram of the loop is shown in Fig. 1c.

The hot section of the loop was simulated by Pipe 100, 110, and 120, among which Pipe 100 was used to simulate the reactor core. Similarly, Pipe 140-160 and Pipe 240-260 were used to simulate the symmetrical cold sections. The heat of the flow was released by the heat exchangers represented by Pipe 150 and 250. To ensure the pressure was maintained at the initial value, pipe structures 300 and 310 and time-dependent control volumes TDV320 were used to simulate the pressurizer for the LBE loop. Meanwhile, to ensure that the number of nodes will not impact the results, the node sensitivity of the key components was calculated[43]. The heating and cooling pipe sections were analyzed, and their nodes were selected as 10.

3. SCALING ANALYSIS OF THE LBE NATURAL CIRCULATION LOOP

3.1. Scaling analysis methods

H2TS and DSS are interesting scaling analysis methods and have been discussed many times in the previous studies[40–42]. However, those analyses were all based on the water loops. To expand its application in the field of LBE natural circulation and guide the design of the scaled-down experimental bench, the above theories were applied to the loop shown in Fig. 1c. The principles of different scaling methods and the treatment of the conservation equations have been comprehensively described in the previous studies[40, 41]. The key steps of each method will be described and the detailed scaling criterion will be shown here.

First, the momentum integral and the energy equations of the loop are given by:

$$\frac{l}{A}\frac{dw}{dt} = \beta_s g \rho H \Delta T - \frac{w^2}{2\rho A^2}\left(\frac{fl}{d} + k\right) \quad (1)$$

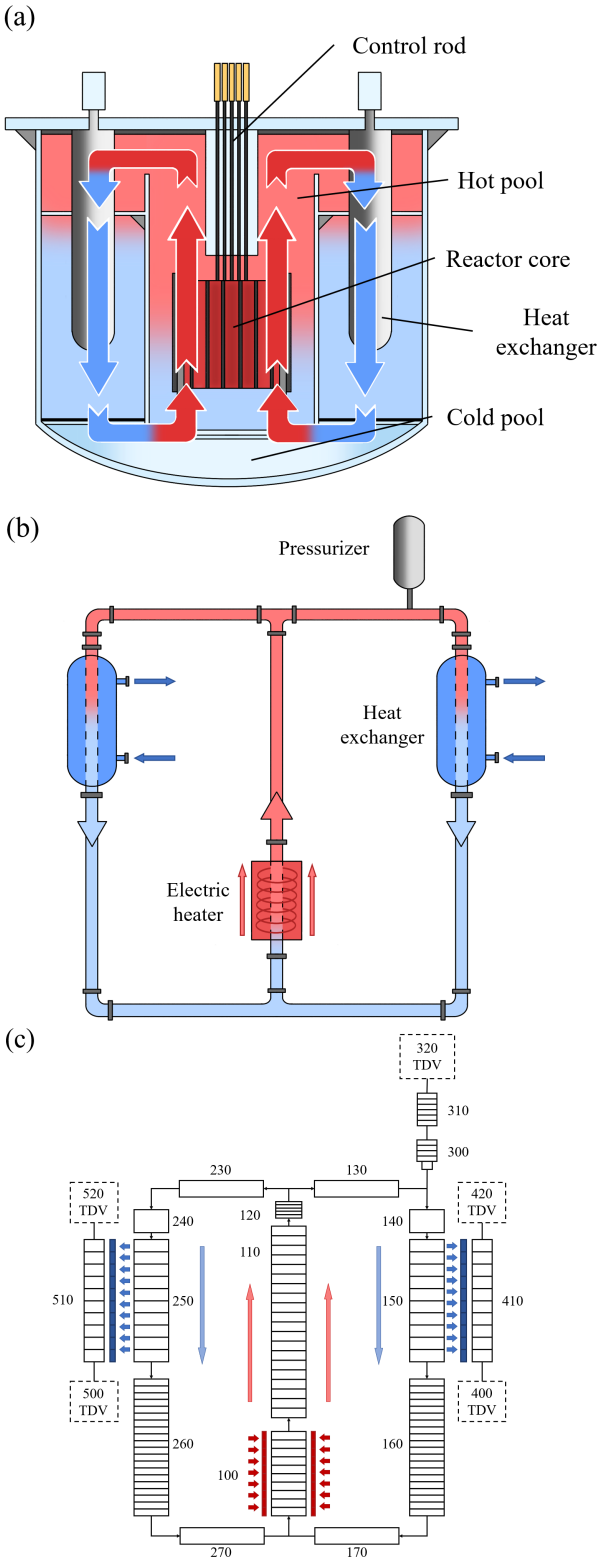

Fig. 1. **a** Schematic of the LBE fast reactor cooling system. **b** The simplified LBE natural circulation loop. **c** Nodalization of the LBE circuits

$$\rho c_p \left(\frac{\partial T}{\partial t} + u \frac{\partial T}{\partial z} \right) = \frac{q\xi}{A} \tag{2}$$

Considering the simplification principle (1) of the model, the energy equation can be simplified to:

$$\rho c_p \left(\frac{\partial T}{\partial t} + u \frac{\partial T}{\partial z} \right) = \frac{4q}{A} \tag{3}$$

Eqs. (1) and (3) have the dimensionless form:

$$\frac{\mathrm{d}u^+}{\mathrm{d}t^+} = \Delta T^+ \frac{\beta_s g H \Delta T_0}{u_0^2} - \frac{1}{2} \left(\frac{fl}{d} + k \right) \left(u^2 \right)^+ \tag{4}$$

$$\frac{\partial T^+}{\partial t^+} + \frac{\partial T^+}{\partial z^+} = \frac{4ql}{\rho c_p u_0 d \Delta T_0} \tag{5}$$

To make the above equations applicable to both the prototype and the scaled-down cases, the following scaling criteria are defined as follows:

$$\prod_{Ri,R} = \left(\frac{\beta_s g H \Delta T_0}{u_0^2} \right)_R = 1 \tag{6}$$

$$\prod_{Fr,R} = \left(\frac{fl}{d} + k \right)_R = 1 \tag{7}$$

$$\prod_{Qs,R} = \left(\frac{4ql}{\rho c_p u_0 d \Delta T_0} \right)_R = 1 \tag{8}$$

Combining Eqs. (6) to (8), the detailed criterion numbers are obtained:

$$d_R = l_R^{\frac{7}{10}}, u_R = l_R^{\frac{1}{2}}, w_R = l_R^{\frac{19}{10}}, Q_R = l_R^{\frac{19}{10}}, \Delta T_R = 1 \tag{9}$$

For the power of the core we have:

$$Q_R = q_R d_R l_R \tag{10}$$

Generally, the H2TS method determines the scaling criteria for the scaled-down loops by combining the key dimensionless criterion numbers. Zhao et al[9]. discussed a steady case of the LBE natural circulation using a similar method. To comprehensively evaluate the different methods, the scaling criterion obtained from the relevant studies is presented here and will be compared in the following discussion.

$$d_R = l_R, u_R = l_R^{\frac{1}{2}}, w_R = l_R^{\frac{5}{2}}, Q_R = l_R^{\frac{5}{2}}, \Delta T_R = 1 \tag{11}$$

Equation (11) shows that Zhao's method has the derivation results similar to those of the H2TS method. The theoretical ratio of the flow velocity and the temperature difference is the same as that in Equation (9). The difference is that the diameter ratio is identical to the length ratio and the two methods have different power ratios of the model cases.

The difference between the DSS and H2TS theories is that the DSS does not analyze individual criterion numbers separately, but instead derives conclusions from the overall conservation equations.

Dimensionless transformation of Eq. (1) and (3) is expressed as:

$$\omega_{w,R}^w = \frac{w_{0,R}}{(Al)_R} \left(\frac{fl}{d} + k \right)_R \left[\frac{w_M^+ (t_M)}{w_P^+ (t_P)} \right]^2 \tag{12}$$

$$\omega_{T,R}^w = \left(\frac{HT_0}{lu_0} \right)_R \left[\frac{T_M^+ (t_M)}{T_P^+ (t_P)} \right] \tag{13}$$

$$\omega_{T,R}^T = \frac{q_R}{A_R \Delta T_{0,R}} \left[\frac{1 - w_M^+ (t_M)}{1 - w_P^+ (t_P)} \right] \tag{14}$$

DSS scaling criteria are as follows:

$$\beta_R = \lambda_A, \omega_R = \lambda_B \tag{15}$$

$$\lambda_R = \tau_{S,R}, \tau_{S,R} = \frac{\lambda_A}{\lambda_B} \tag{16}$$

According to the simplification principles and the method:

$$\lambda_A^w = \frac{w_M^+ (t_M)}{w_P^+ (t_P)}, \lambda_A^T = \frac{T_M^+ (t_M)}{T_P^+ (t_P)} \tag{17}$$

Eqs. (12) to (14) can be expressed as:

$$\tau_{S,R}^w = \frac{1}{\frac{w_{0,R}}{(Al)_R} \left(\frac{fl}{d} + k \right)_R \lambda_A^w} \tag{18}$$

$$\omega_{T,R}^w = \left(\frac{HT_0}{lu_0} \right)_R \lambda_A^T \tag{19}$$

$$\tau_{S,R}^T = \left(\frac{T_0 d}{q} \right)_R \lambda_A^T \tag{20}$$

Therefore, the DSS scaling criteria can be summarized as follows:

$$\begin{aligned} &d_R = \lambda_A^{\frac{8}{5}} \lambda_B^{-\frac{1}{5}} l_R^{\frac{3}{5}}, u_R = \lambda_B l_R, w_R = \lambda_A^{\frac{16}{5}} \lambda_B^{\frac{3}{5}} l_R^{\frac{11}{5}} \\ &Q_R = \lambda_A^{\frac{11}{5}} \lambda_B^{\frac{13}{5}} l_R^{\frac{16}{5}}, \Delta T_R = \lambda_B^2 \lambda_A^{-1} l_R \end{aligned} \tag{21}$$

In the DSS theory, λ_A and λ_B represent the strain parameters on different coordinates. They determine the specific transformation methods. A comparative analysis was conducted using identity and dilation transformations. For the latter, a slightly larger dilation number of 1.25 was selected. Thus, we have respectively: $\lambda_A = \lambda_B$ =1 and $\lambda_A = \lambda_B$ =1.25.

Combining Eqs. (9), (11), and (21), four specific scaling criteria were obtained. The four methods are summarized and numbered to better describe them in the following text and their scaling number groups are shown in Table 2.

3.2. Model cases of LBE natural circulation

The four methods in Table 2 were used to simulate the LBE loop in Fig. 1c with the common length scales of 0.25, 0.5, and 0.75, and the multiple groups of scaled-down cases were obtained. The corresponding scaling standard of each case can be determined by varying the length ratios. Selecting appropriate case parameters is conducive to the design of actual experimental facilities. Fig. 2 shows the similarity criterion curves of each method.

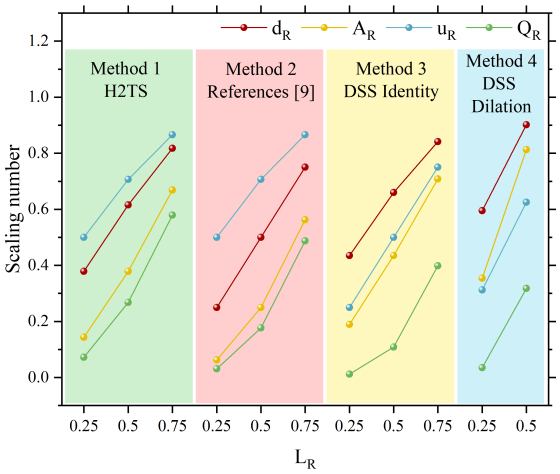

Fig. 2. Scaling number curve with length ratio

For the geometric parameters of the experiment loop, methods 1 and 3 have the similar scaling ratios of the pipe diameter and flow area under all length ratios while the ratios of method 2 are slightly lower. There are obvious differences in method 4. It has the largest diameter and the increase of the ratio is also significantly faster. It should be noted that when $L_R = 0.75$, the corresponding parameters are greater than 1 and this does not conform to the characteristics of scaling. Therefore, the case with $L_R = 0.75$ under method 4 is excluded in the subsequent analysis.

In addition, the power scaling based on method 1 is greater than that of method 2, while method 3 requires a smaller power. Compared with the H2TS method, the smaller lead-bismuth circulation flow rate and power can be obtained using the same length scaling laws and this is one of the features of the DSS methods.

For the design of experimental devices, it is desirable to reproduce the key characteristics of the prototype cases with a smaller size. This helps to save construction costs and improve the economic performance, safety, and flexibility of the experiments, especially for the heavy liquid metal experiments such as LBE. However, the experimental cost does not only include the material cost. An overly small scaled ratio requires higher precision for various control systems in the loop, such as the power adjustment, the circulating flow rate measurement, etc. This may lead to an increase in the expenses. Therefore, when setting the scaled cases, excessive requirements for the control and measurement precision of the facilities should be avoided.

4. RESULTS AND DISCUSSION

4.1. Static errors of the model cases

Firstly, the static errors of the natural circulation under all cases were analyzed. For the convenience of measurement, the focus was on the average mass flow rate and the temperature difference between the hot and cold sections in the LBE loop. Calculate the above parameters of the prototype and model cases respectively under a constant power, and then the actual ratios and the errors can be obtained. The power of the prototype case was set to 20KW based on the design value. The theoretical and actual ratios are shown in Fig. 3a and their errors are shown in Fig. 3b.

It can be seen from Fig. 3 that the static errors of methods 1 and 2 under all length ratios are extremely small. Among them, the deviation of method 2 is slightly larger but still no greater than 5%, which echoes the conclusions of the previous research[9]. For method 3, when the length ratio is 0.5 and 0.75, its errors are also very small, with the maximum being around 5%. The errors are slightly larger when $L_R = 0.25$ and the deviations of both the flow rate and the temperature difference are around 10%. The errors of method 4 are slightly larger but it's still less than 15% under all cases. This may be caused by the differences in physical parameters. The temperature difference of the model cases corresponding to methods 1 and 2 is equal to that of the prototype, while methods 3 and 4 have different temperature ratios. The simulation based on the unequal physical properties of the DSS method may lead to certain static errors.

In general, the actual ratios of the flow rate and temperature difference between the model and prototype cases under the four scaling methods are consistent with the theoretical ratios. Under the steady-state cases of the LBE circulation, the results of the H2TS and DSS methods corroborate each other. If the scaling experiments focus on the static phenomena, all of the above methods are reasonable for the lead-bismuth scaled-down facilities design.

Table 2. Scaling number group based on four scaling methods

Method serial number	Method 1	Method 2	Method 3	Method 4
Description	H2TS	Zhao's method, References[9]	DSS Identity	DSS Dilation, $\lambda = 1.25$
d_R	$l_R^{\frac{7}{10}}$	l_R	$l_R^{\frac{3}{5}}$	$1.367l_R^{\frac{3}{5}}$
u_R	$l_R^{\frac{1}{2}}$	$l_R^{\frac{1}{2}}$	l_R	$1.25l_R$
w_R	$l_R^{\frac{19}{10}}$	$l_R^{\frac{5}{2}}$	$l_R^{\frac{11}{5}}$	$2.335l_R^{\frac{11}{5}}$
Q_R	$l_R^{\frac{19}{10}}$	$l_R^{\frac{5}{2}}$	$l_R^{\frac{16}{5}}$	$2.919l_R^{\frac{16}{5}}$
ΔT_R	1	1	l_R	$1.25l_R$

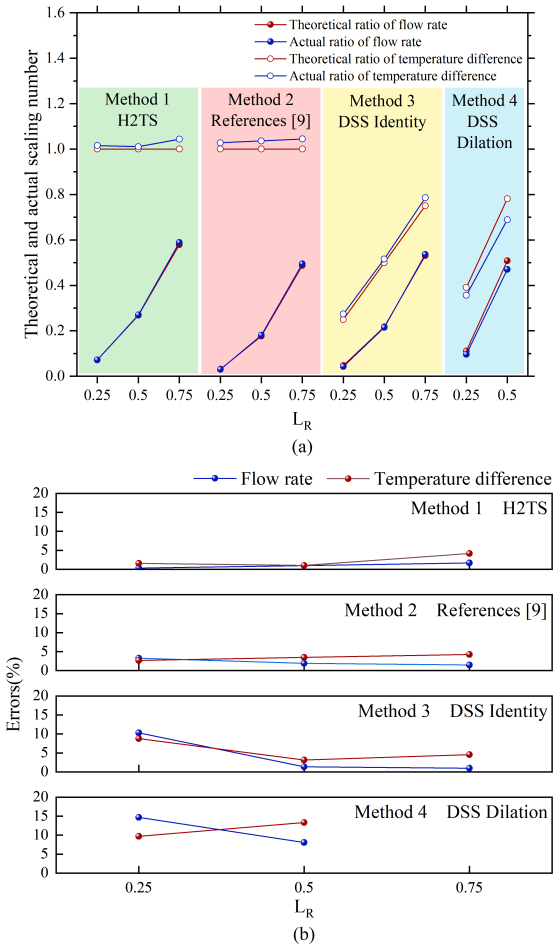

Fig. 3. **a** Theoretical and actual ratio of mass flow rate and temperature difference, **b** Errors in mass flow rate and temperature difference

4.2. Different dynamic cases of LBE natural circulation

For the experimental design, it is reasonable to obtain the dynamic cases by changing the power of the heating section. It is often necessary to conduct the lead-bismuth natural circulation experiments under different transient conditions on a specific device[16, 20]. The scaled-down facility should be able to simulate the prototype's key characteristics under various dynamic cases. Therefore, it is necessary to evaluate the effect of the power change mode on the four scaling methods.

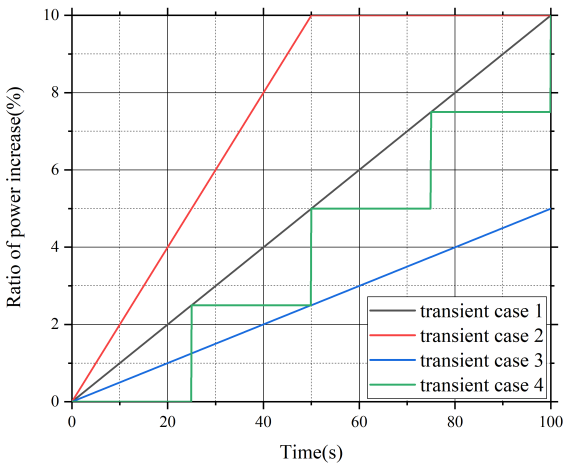

Fig. 4. Cases with different dynamic processes

When the natural circulation reached a steady state under an initial heating power, the power was then increased in four ways to obtain dynamic cases until the circulation became stable again. Based on the initial power value, four different dynamic cases are shown in Fig. 4. In cases 1 and 2, the power was linearly increased by 10% in 100s and 50s. Case 3 had a 5% power increase amplitude, and the power increase rate in case 4 was the same as that in case 1 but had a different change mode. Overall, the above cases discussed the impact of different transient processes on the scaling methods.

Similar to the steady-state analysis, the mass flow rate and temperature difference of the natural circulation were discussed. By fixing the length ratio $L_R = 0.5$, Fig. 5 shows the dynamic curves of different prototypes and scale models, where a-d represents the mass flow rates and e-f represents the temperature differences. To compare all cases uniformly within the same coordinate system, it was necessary to normalize all parameters. For the dimensionless time, the flow rate, and the temperature difference, there were:

$$t^* = \frac{t}{t_0} \tag{22}$$

$$w^* = \frac{w - w_1}{w_2 - w_1} \tag{23}$$

$$\Delta T^* = \frac{\Delta T - \Delta T_1}{\Delta T_2 - \Delta T_1} \tag{24}$$

t_0 in Eq. (22) is the time required for lead-bismuth to complete a cycle in the loop. In Eqs. (23) and (24), the subscripts 1 and 2 represent the values of the corresponding parameters under the initial and the final steady states. Briefly, the processes of all cases are manifested as the changing of the normalized curves from 0 to 1.

Firstly, the mass flow curves for all cases in Figs. 5a-d are discussed. For a fixed length ratio, the prototypes corresponding to all dynamic cases have different flow rate curves, but they were similar in the overall trend. The normalized curves jumped greatly to the maximum value with the increase in the power and then rapidly decreased to a stable range. This change was accomplished within the first cycle of the dynamic process. Subsequently, the flow rate gradually increased at a stable rate until the new state was reached. Cases 1 and 3 have almost the same normalized curves although their powers have different increasing amplitudes: 10% and 5%. The processing time of case 2 is shorter and its curve rose significantly faster. There are deviations between the prototype curves of the different cases and follow the same pattern. There are certain differences in case 4, especially for the initial stage within the first cycle. Slight fluctuations occurred in the flow rate curves of all prototype cases while the model curves corresponding to methods 1 and 2 exhibited significant oscillations that differed greatly from those of the prototype cases. In contrast, the cases corresponding to methods 3 and 4 which belong to the DSS theory reproduced the changing trend of the prototype curves quite well.

Compared with the situation in which the power increases linearly, the fluctuations in the flow rate when the power increases in steps can be easily to explain. It has been demonstrated that the dynamic curves of lead-bismuth cycling are not closely related to the magnitude of power increase but are significantly correlated with the duration of this process. The power was increased by 10% stepwise within 100s in case 4, which can be regarded as four consecutive dynamic processes. Meanwhile, the duration of each of them is very short. This is consistent with the characteristics of the curve fluctuations. The oscillations of the normalized curves of model case 4 in each of Figs. 5a and b also reflect this conclusion. However, case 4 in Figs. 5c and d better agreed with the prototype. This is one of the characteristics of the DSS method, for the distortion of the process time is considered and it is appropriate to evaluate the transient process of the LBE natural circulation.

Figs. 5e-h show the normalized curve of the temperature difference. The conclusions of dynamic cases 1-3 are consistent with the mass flow rate. When the power increased stepped, the temperature difference curves of the prototype and the model cases exhibited the same oscillation process. Apparently, the variation trend of the model curves obtained by the DSS method is more consistent with that of the prototype.

In summary, the scaled models obtained using the above scaling methods can simulate different transient processes when the power changes linearly. The deviations between the models and the prototypes under different dynamic cases are consistent. To further compare diverse scaling methods, such a dynamic process was set. The power increases by 10% linearly in 100 seconds when the natural circulation is steady.

4.3. Transient errors of the certain dynamic cases

Figs. 6a-c respectively show the normalized mass flow rate of the dynamic processes obtained by the four methods under the different length ratios. The curves can be roughly divided into three stages. The flow rate of the prototype case reached 0.98 within approximately 0.7 cycles at the beginning of the power increase and then gradually decreased to 0.9 in the second stage. The curve subsequently increased until it reached the final state and the circulation reached the steady state again within four cycles. Figure 6a shows the cases with $L_R = 0.25$. All the scaled-down cases reached the steady state earlier than the prototype cases and the flow rate curves decreased directly to the final state after increasing rapidly to around 1.05. The differences among the scaling methods are mainly reflected in the initial stage of the transient processes. Cases 1 and 2 showed a distinct retardation in the initial stage, while the curves corresponding to cases 3 and 4 were in better agreement with the prototype. The advantages of the dynamic scaling analysis method are demonstrated especially when the length scale is small.

As the length increases, the deviation of the flow rate curve in the ascending stage gradually decreases. When $L_R = 0.5$, all the scaled cases tended to stabilize within 2.5 cycles. When $L_R = 0.75$, it took 3 cycles which was closer to the prototype. In Figure 6b, the DSS dilation method better restored the decreasing trend of the curve after reaching the maximum value compared with the DSS Identity method. This is consistent with the conclusions of the DSS method in the water model[41]. The scaled-down model cases conform to the prototype case with the increase in the dilation number.

Figure 7 shows the corresponding dynamic errors of each length ratio. The ordinate is defined as:

$$\frac{w_M^* - w_P^*}{w_M^*} \times 100\% \tag{25}$$

As the transient process progresses, the errors of the normalized curves gradually decrease. Moreover, the deviations under different cases are all less than 5% in the second cycle and steadily tend to 0 around the fourth cycle. The four methods differ mainly in the first cycle when the length ratio is fixed. The errors of methods 3 and 4 are both less than 15% in almost all stages of the dynamic process. The errors of the other methods are significantly larger, especially when the length ratio is small. This is similar to the conclusion in

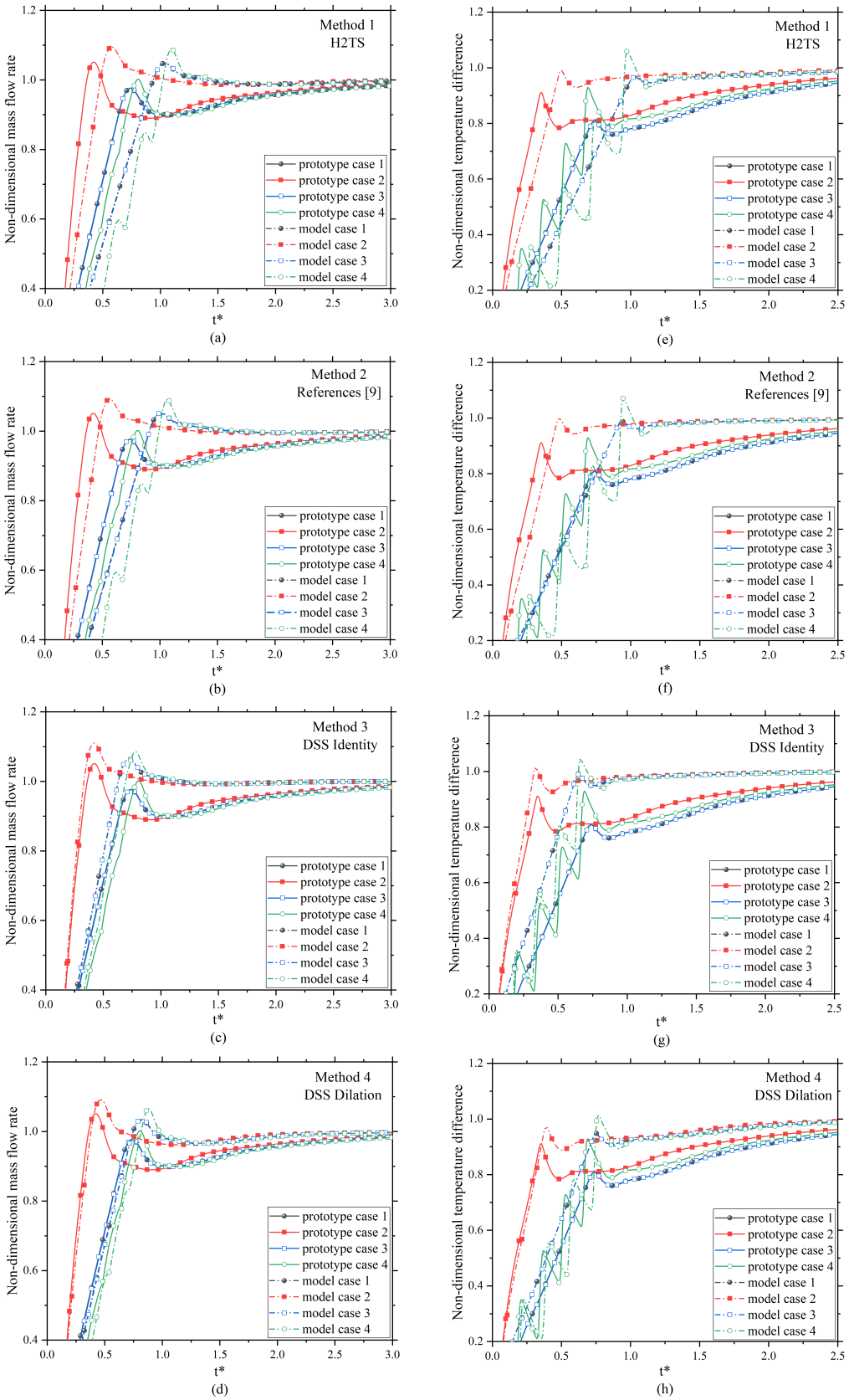

Fig. 5. Transient curve based on different scaling methods **a-d** Normalized mass flow rate **e-h** Normalized temperature difference

Figure 6. Comparing Figs. 7a-c, the dynamic deviation decreases as the length ratio increases and this phenomenon is

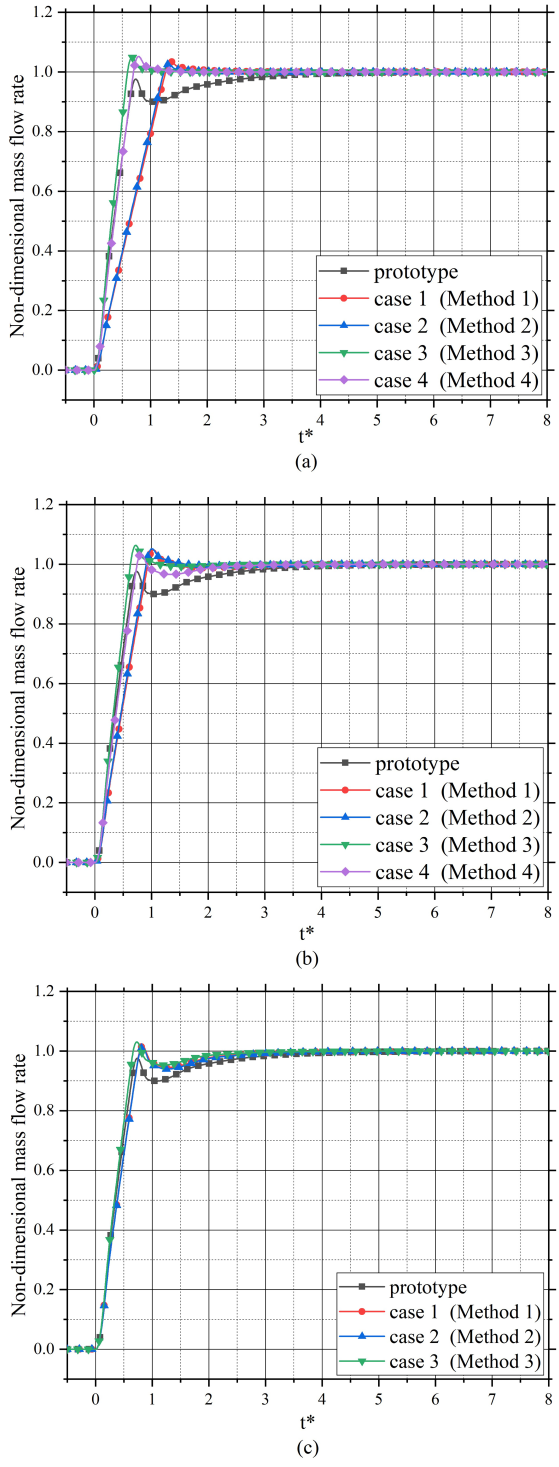

Fig. 6. Transient mass flow rate curves. **a** Length ratio $L_R = 0.25$, **b** Length ratio $L_R = 0.5$, **c** Length ratio $L_R = 0.75$

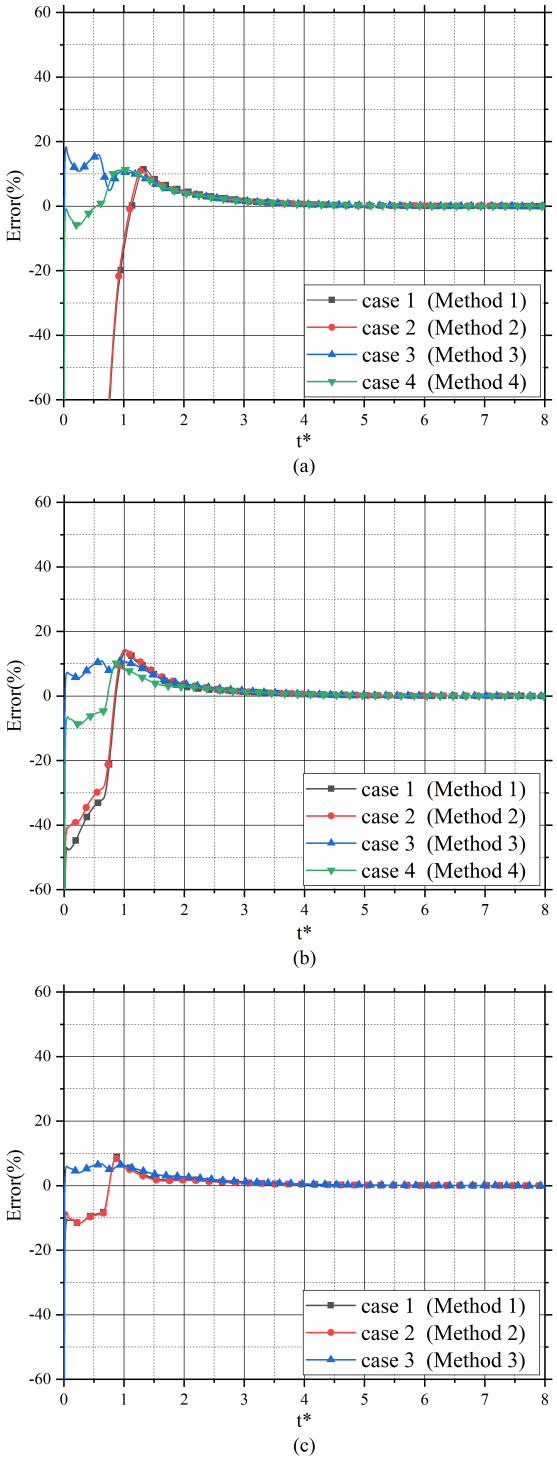

Fig. 7. Relative error of the mass flow rate. **a** Length ratio $L_R = 0.25$, **b** Length ratio $L_R = 0.5$, **c** Length ratio $L_R = 0.75$

even more significant in methods 1 and 2.

Figures 8- 9 show the temperature difference and their relative errors of the LBE circulation. The prototype temperature difference rapidly reached 0.8 when the transient process began. After a slight oscillation, the curves gradually reached the final state in about 4 cycles. When $L_R = 0.25$, the time to get the steady state in the model is less than that in the prototype as shown in Fig. 8a. As shown in Fig. 9a, the main dynamic deviation occurs within the first cycle after the power change. Besides, the errors of all cases are very close and are

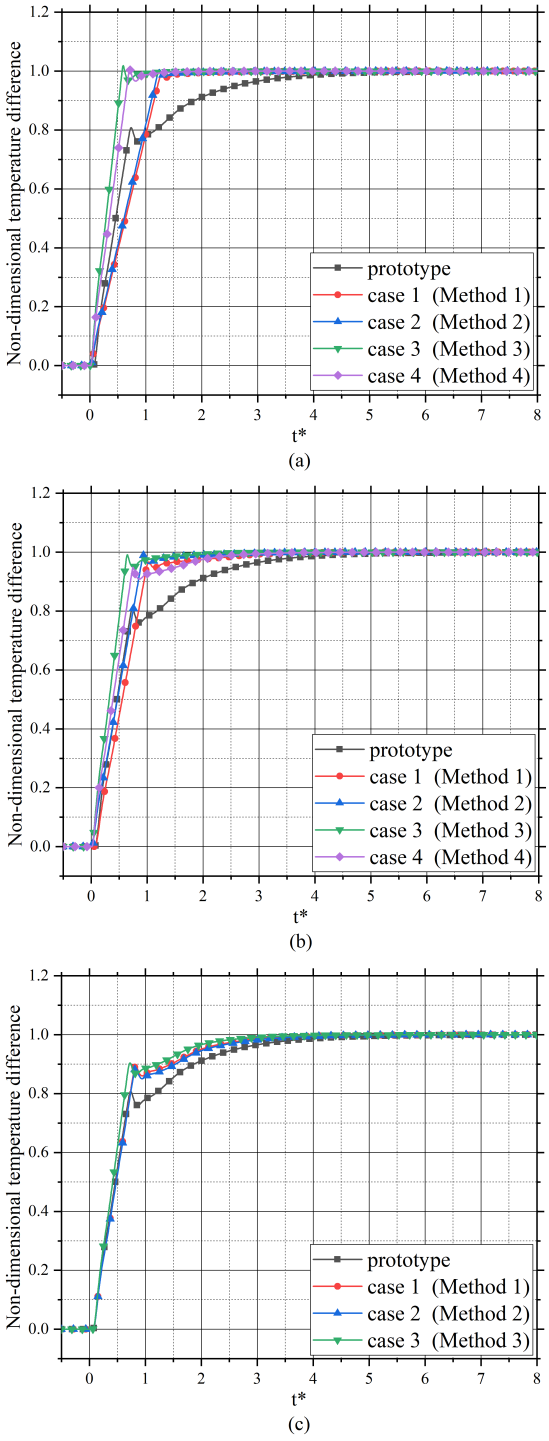

Fig. 8. Transient temperature difference curves. **a** Length ratio $L_R = 0.25$, **b** Length ratio $L_R = 0.5$, **c** Length ratio $L_R = 0.75$

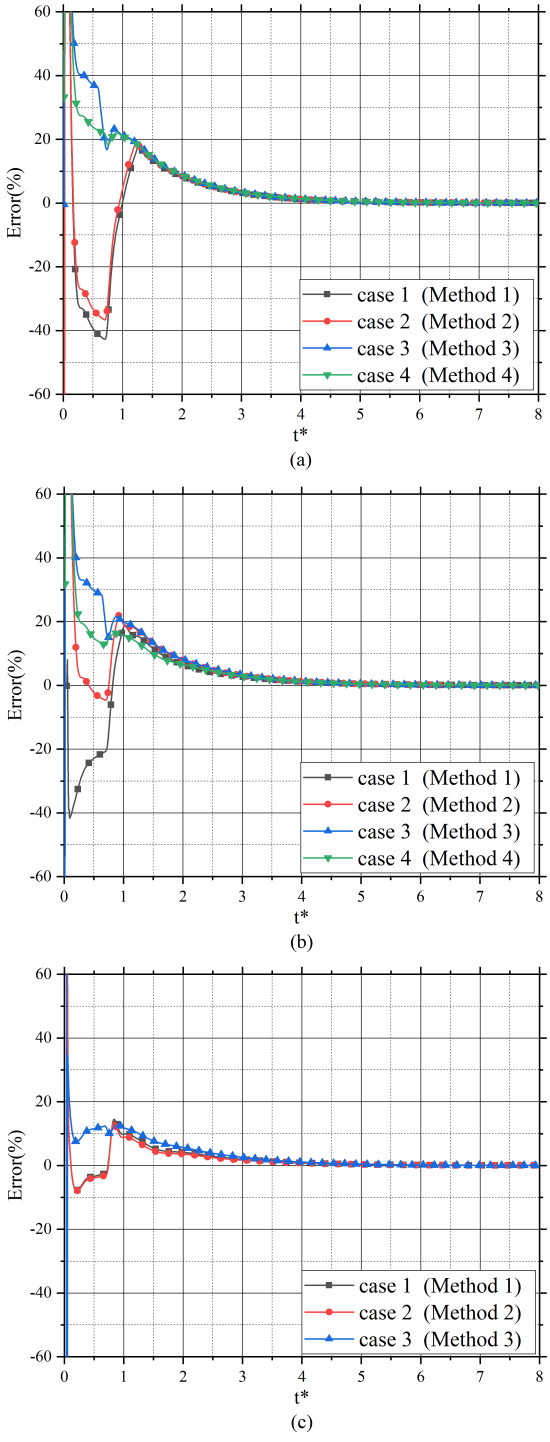

Fig. 9. Relative error of the temperature difference. **a** Length ratio $L_R = 0.25$, **b** Length ratio $L_R = 0.5$, **c** Length ratio $L_R = 0.75$

all less than 10% after the second cycle.

When a moderate length ratio is chosen (Figs. 8b, 9b), the difference between the temperature difference in the initial stage and that of the prototype decreases significantly. The curve of case 4 is more similar to that of the prototype after the second cycle and the conclusion is similar to that for the flow rate. Figs. 8c and 9c show the cases with the length ratio $L_R = 0.75$. The temperature difference curves of all scaled-down cases are close to each other and their trends are similar to those of the prototype case. Even in the initial stage, the

dynamic errors of all cases are within 15% and all the scaling methods are effective.

5. CONCLUSIONS

Based on the natural circulation within the lead-bismuth loop, a prototype case was established by using the Relap5 code. The scaled-down cases are obtained by the H2TS, DSS identity, and DSS dilation methods. The single-phase natural circulation of the LBE was analyzed and the static and dynamic deviations of the characteristic parameters were calculated. The applicability of traditional scaling methods under transient conditions was evaluated and the differences between those methods were compared. The following conclusions were drawn:

(1) Multiple similarity criterion arrays based on the single-phase natural circulation of LBE were deduced. The criterion obtained using the DSS identity method has a similar flow area ratio and corresponds to smaller power. To design the scaled facilities, the impacts of both material and measurement costs should be considered simultaneously.

(2) The H2TS and DSS methods can still be used for the scaling analysis of the static LBE natural circulation. The static errors in the mass flow rate and the temperature are significantly small. The maximum relative deviation of the H2TS method is within 5% while the errors of the DSS identity and dilation methods are less than 10% and 15%. This indicates that all of the methods are feasible and the H2TS method has a slightly greater advantage under the static conditions because of the simulation based on the equal physical properties.

(3) The deviations between the scaled-down and the prototype cases are similar under the different transient conditions when the power changes linearly for each scaling method. Therefore, the scaled facility can carry out various natural circulation transient experiments. The models based on different methods can simulate the trends of the characteristic parameters of the LBE natural circulation under the prototype case. The cases obtained with the DSS methods fit the initial stage of the prototype more accurately than those of the H2TS method when the length ratio is small. As the length ratio increases, the differences among various methods gradually decrease, and the model cases gradually conform to the prototype case. If the power changes nonlinearly, the DSS method can better restore the transient characteristics of the prototype cases while the H2TS method has obvious deviations. This indicates that the outstanding advantages of the DSS theory are also applicable to the flow of LBE.

Future work will be carried out from the following two aspects. The scaled experimental facility will be established and the natural circulation phenomena will be further studied. The influence of the complex internal structure in the pool-type reactor on the scaling methods will be discussed.

6. ACKNOWLEDGEMENTS

The authors highly regard the efforts of group members and the numerical computations were performed on Hefei advanced computing center.

[1] J. R. Weeks, Lead, bismuth, tin and their alloys as nuclear coolants. Nucl. Eng. Des. **15**, 363-372 (1971). doi: 10.1016/0029-5493(71)90075-6

[2] Y. Lu, J. He, Z. Q. Zhu et al., Preliminary calibration test and analysis of electromagnetic flow-meter in liquid lead-bismuth. Nucl. Tech. **37**, 77-82 (2014). doi: j.0253-3219.2014.hjs.37.080603(in Chinese)

[3] Z. J. Deng, S. B. Cheng, H. Cheng, Experimental investigation on pressure-buildup characteristics of a water lump immerged in a molten lead pool. Nucl. Sci. Tech. **34**, 1-15 (2023). doi: 10.1007/s41365-023-01188-1

[4] Y. X. Li, R. S. Yang, Y. Li et al., Study on the thermo-hydraulic behaviors of the new-pattern fuel assembly in lead-based fast reactors based on OpenFOAM. Nucl. Sci. Tech. **35**, 181 (2024). doi: 10.1007/s41365-024-01560-9

[5] Y. X. Li, L. Meng, S. Li et al., CFD analysis of a CiADS fuel assembly during the steam generator tube rupture accident based on the LBEsteamEulerFoam. Nucl. Sci. Tech. **34(10)**, 136-147 (2023). doi: 10.1007/s41365-023-01312-1

[6] J. He, Q. Y. Huang, Z. Q. Zhu et al., Experiment and analysis on flow rate and temperature of liquid PbBi in PREKY. Nucl. Sci. Tech. **26(1)** (2015). doi: 10.1007/s41365-016-0036-3

[7] F. Bianchi, C. Artioli, K. W. Burn et al., Status and trend of core design activities for heavy metal cooled accelerator driven system. Energ. Convers. Manage. **47(17)**, 2698-270912 (2006). doi: 10.1016/j.enconman.2006.02.005

[8] T. L. Schulz, Westinghouse AP1000 advanced passive plant. Nucl. Eng. Des. **236**(14-16), 1547-1557 (2006). doi: 10.1016/j.nucengdes.2006.03.049

[9] P. C. Zhao, E. P. Zhu, H. X. Yu et al., Research on Scaling Analysis Method for Natural Circulation Test Facility of Lead-Based Fast Reactor. Nuclear Power Engineering. **41(06)**, 207-213 (2020). doi: 10.13832/j.jnpe.2020.06.0207(in Chinese)

[10] P. C. Zhao, T. Wang, E. P. Zhu et al., Research on proportional method for experimental facility of lead-based fast reactor with natural circulation. Ann. Nucl. Energy. **172**, 109096 (2020). doi: 10.1016/j.anucene.2022.109096

[11] Y. H. Shin, S. Choi, J. Cho et al., Advanced passive design of small modular reactor cooled by heavy liquid metal natural circulation. Prog. Nucl. Energ. **83**, 433-442 (2015). doi: 10.1016/j.pnucene.2015.01.002

[12] C. Zeng, C. Shen, X. Jin et al., Transient thermal hydraulic analysis of a small passive lead-bismuth eutectic cooled fast reactor. Ann. Nucl. Energy. **210**, 110884 (2025). doi: 10.1016/j.anucene.2024.110884

[13] H. L. Chen, Z. Chen, T. Zhou et al., Preliminary Thermal-hydraulic Design and Analysis of China Lead Alloy Cooled Research Reactor (CLEAR-I). Proceedings of the 9th International Topical Meeting on Nuclear Thermal-Hydraulics, Operation and Safety (NUTHOS-9'12). 1-9 (2012).

[14] W. M. Ma, A. Karbojian, B. R. Sehgal, Experimental study on natural circulation and its stability in a heavy liquid metal

loop. Nucl. Eng. Des. **237**(15-17), 1838-1847 (2007). doi: 10.1016/j.nucengdes.2007.02.023

[15] P. Agostini, G. Bertacci, G. Gherardi et al., Natural Circulation of Lead-Bismuth in a One-Dimensional Loop: Experiments and Code Predictions. International Conference on Nuclear Engineering. 35960, 755-761 (2002). doi: 10.1115/ICONE10-22356

[16] G. Coccoluto, P. Gaggini, V. Labanti et al., Heavy liquid metal natural circulation in a one-dimensional loop. Nucl. Eng. Des. **241(5)**, 1301-1309 (2011). doi: 10.1016/j.nucengdes.2010.06.048.

[17] Y. Li, K. F. Lv, L. L. Chen et al., Experiments and analysis on LBE steady natural circulation in a rectangular shape loop. Prog. Nucl. Energ. **81**, 239-244 (2015). doi: 10.1016/j.pnucene.2014.12.009

[18] G. M. Ran, Q. Y. Huang, S. Gao, Preliminary Design and Analysis of a Lead-Bismuth Natural Circulation Loop. International Conference on Nuclear Engineering. American Society of Mechanical Engineers, 55812 (2013). doi: 10.1115/ICONE21-16568

[19] L. T. Shi, T. Bing, C. L. Wang et al., Experimental investigation of gas lift pump in a lead-bismuth eutectic loop. Nucl. Eng. Des. **330**, 516-523 (2018). doi: 10.1016/j.nucengdes.2018.01.042

[20] L. T. Shi, G. H. Su, F. J. Zhu et al., Experimental study on the natural circulation capability and heat transfer characteristic of liquid lead bismuth eutectic. Prog. Nucl. Energ. **115**, 99-106 (2019). doi: 10.1016/j.pnucene.2019.03.003

[21] W. S. Duan, Z. R. Zou, X. Luo et al., Startup scheme optimization and flow instability of natural circulation lead-cooled fast reactor SNCLFR-100. Nucl. Sci. Tech. **32**, 133 (2021). doi: 10.1007/s41365-021-00970-3

[22] Q. Y. Yu, J. W. Qi, P. C. Zhao et al., Uncertainty analysis of unprotected transient overpower of small natural circulation lead-bismuth cooled fast reactor. Nucl. Tech. **45**,080604 (2022). doi: 10.11889/j.0253-3219.2022.hjs.45.080604

[23] S. Grewal. E. Gluekler. Water simulation of sodium reactors. Chem. Eng. Commun. **17**(1-6), 343-360 (1982). doi: 10.1080/00986448208911637

[24] P. Planquart. K. V. Tichelen, Experimental investigation of accidental scenarios using a scale water model of a HLM reactor. Nucl. Eng. Des. **346**, 10-16 (2019). doi:10.1016/j.nucengdes.2019.02.016

[25] X. N. Chen, On LBE natural convection and its water experimental simulation. Prog. Nucl. Energ. **78**, 372-379 (2015). doi:10.1016/j.pnucene.2014.03.001

[26] C. Deng, X. Zhang, Y. Yang et al., Research on scaling design and applicability evaluation of integral thermal-hydraulic test facilities: a review. Ann. Nucl. Energy **131**, 273-290 (2019). doi:10.1016/j.anucene.2019.03.042

[27] S. M. Modro, S. N. Aksan, V. T. Berta et al., Review of LOFT (Loss-of-fluid test) large break experiments. Nucl. Regul. Comm. (1989). doi:10.2172/5497189

[28] M. T. Friend, R. F. Wright, R. Hundal et al., Simulated AP600 response to small-break loss-of-coolant-accident and non-loss-ofcoolant-accident events: analysis of SPES-2 Integral test results. Nucl. Technol. **122**, 19-42 (1998). doi:10.13182/ NT98-A2848

[29] P. K. Vijayan, H. Austregesilo, Scaling laws for single-phase natural circulation loops. Nucl. Eng. Des. **152**(1-3), 331-347 (1994). doi:10.1016/0029-5493(94)90095-7

[30] H. J. Yoon, S. T. Revankar, Y. Xu et al., Design and test of hydraulic vacuum breaker check valve for simplified boiling water reactor. Nucl. Eng. Des. **236**, 2405-2410 (2006). doi:10.1016/j.nucengdes.2006.02.013

[31] M. Ishii, S.T. Revankar, T. Leonardi et al., The three-level scaling approach with application to the Purdue University multi-dimensional integral test assembly (PUMA). Nucl. Eng. Des. **186**, 177-211 (1998). doi:10.1016/S0029-5493(98) 00222-2

[32] W. P. Baek, C. H. Song, B. J. Yun, KAERI integral effect test program and the ATLAS design. Nucl. Technol. **152**(2), 183-195 (2005). doi:10.13182/NT05-A3669

[33] N. Zuber, G. E. Wilson, M. Ishii et al., An integrated structure and scaling methodology for severe accident technical issue resolution: development of methodology. Nucl. Eng. Des. **186**, 1-21 (1998). doi:10.1016/S0029-5493(98)00215-5

[34] Y. S. Liu, S. C. Tan, J. P. Jing et al., Investigation on natural circulation phenomena of LOCA with PRHR, pipeline break in ACME facility. Nucl. Tech. **46**, 060601 (2023). doi:10.11889/j.0253-3219.2023.hjs.46.060601 (in Chinese)

[35] N. Zuber, U.S. Rohatgi, W. Wulff et al., Application of fractional scaling analysis (FSA) to loss of coolant accidents (LOCA). Nucl. Eng. Des. **237**, 1593-1607 (2007). doi:10.1016/j.nucengdes.2007.01.017

[36] J. Reyes, The dynamical system scaling methodology, In: Proceeding of the 16th International Topical Meeting on Nuclear Reactor Thermal Hydraulics (NURETH-16), (2015)

[37] X. B. Li, N. Li, Q. Wu et al., Application of dynamical system scaling method on simple gravity-driven draining process. Nucl. Sci. Technol. **55**, 11-18 (2017). doi:10.1080/00223131.2017.1372231

[38] X. B. Li, B. T. Zhan, Y. S. Liu et al., Dynamic characteristics and scaling distortion of gravity-driven draining process in core makeup tank. Ann. Nucl. Energy. **151**(4), 107963 (2021). doi:10.1016/j.anucene.2020.107963

[39] X. B. Li, H. Y. Li, Y. S. Liu et al., Numerical scaling assessment on natural circulation in Core Makeup Tank. Ann. Nucl. Energy. **140**, 107105 (2020). doi:10.1016/j.anucene.2019.107105

[40] X. B. Li, H.Y. Li, N. Li et al., DSS application on single-phase natural circulation in a simple rectangular loop. Ann. Nucl. Energy. **119**, 214-228 (2018). doi:10.1016/j.anucene.2018.05.004

[41] J. N. Xu, X. B. Li, Y. S. Liu et al., Two-parameter dynamical scaling analysis of single-phase natural circulation in a simple rectangular loop based on dilation transformation. Nucl. Sci. Tech. **33**, 156 (2022). doi:10.1007/s41365-022-01138-3

[42] J. N. Xu, X. B. Li, Z. Y. Wang et al., Dynamic scaling characteristics of single-phase natural circulation based on different strain transformations. Nucl. Sci. Tech. **34**(9), 142 (2023). doi:10.1007/s41365-023-01296-y

[43] R. Urbonas, E. Uspuras, A. Kaliatka, State-of-the-art computer code RELAP5 validation with RBMK-related separate phenomena data. Nucl. Eng. Des. **225**, 65-81 (2003). doi:10.1016/S0029-5493(03)00150-X